

Investigation of the shape of uranium in relativistic $^{238}\text{U}+^{238}\text{U}$ collisions with nuclear densities from covariant density functional theory

Yuan Li,^{1,2,3} Hao-jie Xu,^{2,3,4,*} Dandan Zhang,^{5,†} and Guo-Liang Ma^{1,3,‡}

¹*Key Laboratory of Nuclear Physics and Ion-beam Application (MOE), Institute of Modern Physics, Fudan University, Shanghai 200433, China*

²*School of Science, Huzhou University, Huzhou, Zhejiang 313000, China*

³*Shanghai Research Center for Theoretical Nuclear Physics, NSFC and Fudan University, Shanghai 200438, China.*

⁴*Strong-Coupling Physics International Research Laboratory (SPiRL), Huzhou University, Huzhou, Zhejiang 313000, China.*

⁵*Institute of Theoretical Physics, Chinese Academy of Science, Beijing 100871, China*

Relativistic $^{238}\text{U}+^{238}\text{U}$ collisions have recently been used to extract the quadrupole shape of ^{238}U . In this study, we employ state-of-the-art three-dimensional (3D) lattice covariant density functional theory (CDFT) with pairing correlations to calculate the density of uranium, including its octupole and hexadecapole deformations, as input for hydrodynamic simulations of these collisions. We find that while the CDFT density well describes elliptic flow, a clear mismatch emerges with transverse-momentum-related observables, indicating a tension in the effective quadrupole deformation. Furthermore, constraining the octupole deformation with triangular flow v_3 proves to be difficult due to significant sensitivity to the uncertain nuclear structure of the gold reference system. Our results underscore the necessity of realistic nuclear densities for both colliding species and highlight the need for further investigation of correlations related to both flow and transverse momentum to fully characterize nuclear deformation.

I. INTRODUCTION

Uranium-Uranium collisions have attracted wide interest in both low-energy nuclear reactions and high-energy heavy ion collisions [1–20]. Such collisions have been considered as important candidates for the production of actinides and super-heavy elements, as well as for the isolation of the background in chiral magnetic effect search [6, 21, 22]. In these studies, the pronounced shape deformation (denoted as β_n) of ^{238}U contributes significantly to collision dynamics and thus to the observables [9–11, 18, 19]. Although quadrupole deformation (characterized by a well-measured ground-state electric transition rate $B(E2) = 12.09 \pm 0.20 \text{ e}^2\text{b}^2$) is firmly established, higher-order deformations of ^{238}U , such as octupole and hexadecapole deformations, remain challenging to be quantified both experimentally and theoretically [23].

The density functional theory (DFT) is the standard theoretical framework for calculating the density profile of ^{238}U . Despite considerable uncertainties, DFT calculations consistently predict a substantial hexadecapole deformation in the ground state of ^{238}U . Recent studies also propose a modest softness octupole deformation that arises not from static shape deformation but from collective vibrational modes [24–27]. A time-dependent covariant density functional theory (TD-CDFT) simulation found the critical influence of the octupole deformation on the ternary quasi-fission process observed in low-energy $^{238}\text{U}+^{238}\text{U}$ collisions, providing a way to determine the octupole deformation of the colliding nuclei [28].

The shape of uranium can also be determined from relativistic heavy ion collisions. In relativistic heavy ion colli-

sions, the pressure gradient of the quark gluon plasma (QGP) converts the spatial anisotropy of the initial geometry (eccentricity ϵ_n) of the overlap region into the momentum anisotropy (anisotropic flow v_n) of the final state hadrons [29–32]. In the most central collisions, the overlap geometry is essentially determined by the shape of the colliding nuclei once their deformation is large enough to emerge from the contributions of fluctuations driven by the finite number of colliding nuclei [33]. With the $v_n^2 \propto \beta_n^2$ ($n = 2, 3$) connection, one can in principle extract the deformation parameter from the heavy ion data, and this has been reported by the STAR Collaboration for the quadrupole deformation of ^{238}U [19]. This is a direct measurement of the shape of the ground state ^{238}U , since the interaction time of the incoming nuclei is only few yoctosecond (10^{-24}s), much shorter than the timescale of low-energy nuclear reactions.

Besides the anisotropic flow, multiparticle correlations in heavy ion collisions provide deeper insights into the shape of the colliding nuclei. For example, the three-particle correlations are uniquely sensitive to both quadrupole and hexadecapole deformations. Recent studies also emphasize that mismatch in the definition of deformations is critical to resolving the discrepancies between high-energy heavy ion observables and low-energy nuclear structure expectations [12–15]. For a more quantitatively accurate analysis, it is crucial to employ a reliable nuclear density distribution, obtained from or constrained by DFT calculations, as input for heavy-ion collision simulations in this type of interdisciplinary investigation. The continued use of a simple Woods-Saxon density profile has already led to ambiguities within the community, particularly regarding the interpretation of v_2 ratios in $^{238}\text{U}+^{238}\text{U}$ versus $^{197}\text{Au}+^{197}\text{Au}$ collisions [14, 15, 18], as well as in the estimation of background contributions in relativistic isobar collisions [21, 22].

In this work, we investigate the effect of quadrupole (β_2) and

* haojiexu@zjhu.edu.cn

† ddzhang@itp.ac.cn

‡ glma@fudan.edu.cn

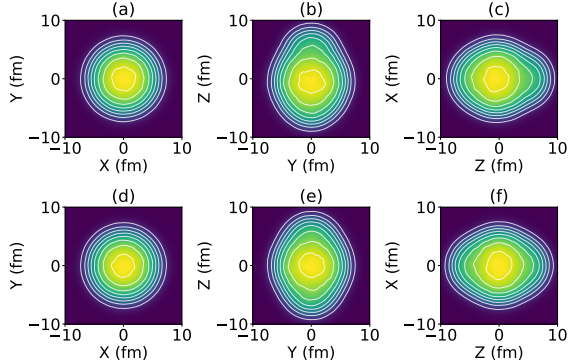


FIG. 1. (Color online) Density distributions of ^{238}U obtained from covariant density functional theory calculations for an octupole-deformed configuration ($\beta_{20} = 0.29$, $\beta_{30} = 0.09$, upper panels (a)–(c)) and the corresponding purely prolate configuration ($\beta_{20} = 0.29$, $\beta_{30} = 0$, lower panels (d)–(f)).

octupole deformation (β_3) on collective dynamics in relativistic $^{238}\text{U}+^{238}\text{U}$ collisions at $\sqrt{s_{\text{NN}}} = 200$ GeV, using state-of-the-art hydrodynamic simulations that incorporate the nuclear density obtained from CDFT calculations. The paper is organized as follows. Section II gives a brief introduction to the model and the DFT framework used in this work. Section III discusses the effect of octupole deformation of uranium and the variations in shape configuration and the Woods–Saxon parameters, on observables in relativistic $^{238}\text{U}+^{238}\text{U}$ collisions and $^{197}\text{Au}+^{197}\text{Au}$ collisions. A summary is given in Sect. IV.

II. MODEL AND SETUPS

In this study, $^{238}\text{U}+^{238}\text{U}$ collisions are simulated by the event-by-event (2+1)-dimensional viscous hydrodynamic model iEBE-VISHNU [34–37] to describe the dynamic evolution of the QGP medium, together with the hadron cascade UrQMD model to simulate that of the subsequent hadronic matter [38, 39]. The initial condition of the collisions is obtained by the TRNTO model [37, 40], given a nuclear density distribution. All parameters for the iEBE-VISHNU simulations are taken from [41], except the normalization factor to match the multiplicity.

The point-coupling relativistic energy density functional PC-PK1 is used for nuclear density calculations. The density profiles for the ground state of ^{238}U are obtained using covariant density functional theory (CDFT) in a three-dimensional (3D) lattice space with $L_x \times L_y \times L_z = 24 \times 24 \times 30$ fm 3 . The deformation parameters of the equilibrium minimum are $\beta_{20} = 0.29$ and $\beta_{30} = 0.09$ ¹, which are referred to as the octupole state. To investigate the effect of the octupole deformation, we compared it with simulations with the density

at the energy minimum along the $\beta_{30} = 0$ direction, termed the quadrupole prolate state. For a comprehensive description of the CDFT calculations, we refer the reader to Ref. [28]. The density profiles of ^{238}U exhibit pronounced differences between the octupole and prolate deformations, as illustrated in Fig. 1.

For each case of $^{238}\text{U}+^{238}\text{U}$ and $^{197}\text{Au}+^{197}\text{Au}$ collisions, approximately 10^6 hydrodynamic events are generated, with each event followed by 10 oversamplings using the UrQMD afterburner. The flow observables are calculated using both the standard Q-cumulant method [42, 43] and the pseudorapidity-separated sub-event method, which are found to yield consistent results. The standard Q-cumulant method is applied to charged particles with transverse momentum $0.2 < p_T < 2$ GeV/c and pseudorapidity $|\eta| < 2$.

Before discussing the results, we now give some definitions of the observables. The flow and flow correlations are calculated using the multi-particle cumulants method with

$$v_n\{2\} \equiv \sqrt{c_n\{2\}} \equiv \sqrt{\langle\langle 2 \rangle\rangle_{n,-n}}, \quad (1a)$$

$$\begin{aligned} \langle v_n^2 \delta p_T \rangle &\equiv \text{Cov}(v_n^2, [p_T]) \\ &= \langle v_n^2 [p_T] \rangle - \langle v_n^2 \rangle \langle [p_T] \rangle, \end{aligned} \quad (1b)$$

respectively, where $\langle\langle m \rangle\rangle_{n_1, n_2, \dots, n_m}$ represents the correlator,

$$\langle\langle m \rangle\rangle_{n_1, n_2, \dots, n_m} \equiv \langle e^{i(n_1 \varphi_1 + n_2 \varphi_2 + \dots + n_m \varphi_m)} \rangle. \quad (2)$$

The quantities are averaged over the particles of interest (POIs) within an event by the inner $\langle \dots \rangle$, and over all events by the outer $\langle \dots \rangle$ [42, 43]. The event-averaged transverse momentum is denoted by $[p_T]$, and $\text{Cov}(v_n^2, [p_T])$ represents the covariance between v_n^2 and $[p_T]$. In addition to $\langle v_n^2 \delta p_T \rangle$, the variance of $[p_T]$, $\langle (\delta p_T)^2 \rangle \equiv \sigma_{p_T}^2$, is also sensitive to nuclear deformation effects [44–46]. Here, $\delta p_T = [p_T] - \langle [p_T] \rangle_{\text{event}}$ is the fluctuation of $[p_T]$ in a given centrality range, and $\langle \dots \rangle$ denotes the average over an ensemble of events.

TABLE I. Deformation parameters employed for ^{197}Au in the present analysis. The parameter sets $\text{Au}_{\text{default}}$ and Au_{new} correspond to distinct Woods–Saxon configurations for Au, as detailed in the text.

Configurations	R_0 (fm)	a (fm)	β_2^{WS}	β_4^{WS}
$\text{Au}_{\text{default}}$ [19]	6.38	0.535	-0.14	0.00
Au_{new} [13]	6.42	0.410	-0.14	0.00

The mapping from nuclear deformation to final-state observables is influenced by the evolution of the medium produced in relativistic heavy ion collisions, which introduces theoretical uncertainties. These uncertainties can be mitigated by comparing similar collision systems, where many systematic effects are largely canceled. A prominent example is the isobaric Ru+Ru and Zr+Zr collisions [21, 47, 48]. In this work, we use Au+Au collisions as a reference for U+U collisions and construct relative observables,

$$R(X) = \frac{X_{\text{UU}}}{X_{\text{AuAu}}}, \quad (3)$$

¹ We emphasize that these deformation parameters differ from those employed in conventional Woods–Saxon parameterizations. The latter will be denoted by β^{WS} .

where X stands for a given observable, e.g. $v_n^2\{2\}$, $\langle v_2^2 \delta p_T \rangle$ or $\langle (\delta p_T)^2 \rangle$. In principle, for simulations of $^{197}\text{Au} + ^{197}\text{Au}$ collisions, the density profile for ^{197}Au should be calculated with the CDFT framework. However, due to the complex nature of even-odd nucleus, we just adopt the Woods-Saxon profiles for ^{197}Au in this study, and the parameters are listed in Tab. I. We emphasize that, as will be demonstrated below, an accurate specification of the nuclear density distribution of ^{197}Au is crucial for a reliable description of the observables associated with $R(X)$, in particular for capturing their centrality dependence.

III. RESULTS AND DISCUSSIONS

Figure 2(a) shows the ratio of $v_2\{2\}^2$ between $\text{U} + \text{U}$ and $\text{Au} + \text{Au}$ collisions for different uranium deformation configurations. Symbols and curves represent the final-state flow ratio $R(v_2\{2\}^2)$ and the initial-state eccentricity ratio $R(\varepsilon_2^2)$, respectively. The initial-state TRDENTo and final-state iEBE-VISHNU results show excellent agreement for the top 20% centrality range, validating the linear response in this regime. It is well established that v_2 differences in central collisions are predominantly driven by quadrupole deformation β_2 [33]. For uranium, CDFT calculations with and without octupole deformation yield the same quadrupole deformation value $\beta_{20} = 0.29$. Consequently, $\text{U}_{\text{octupole}}$ (red triangles) and $\text{U}_{\text{prolate}}$ (blue squares) show no significant differences in $R(v_2\{2\}^2)$.

Although the numerical values are identical, the CDFT prediction $\beta_{20} = 0.29$ [28] and the Woods-Saxon deformation parameter $\beta_2^{\text{WS}} = 0.29$ correspond to physically different quadrupole deformations [14, 15]. In our CDFT calculations, the presence of a finite hexadecapole deformation ($\beta_{40} = 0.16$) leads to an effective Woods-Saxon quadrupole parameter β_2^{WS} that is substantially smaller than the intrinsic value β_{20} [14, 15]. Consequently, the so-called ultra-central v_2 puzzle, namely the pronounced overestimation of $R(v_2\{2\}^2)$, is largely resolved within our simulations. Furthermore, we find that the commonly employed parameter set for Au induces a clear and systematic overestimation of the magnitude of $R(v_2\{2\}^2)$ by approximately 0.1, as illustrated in Fig. 2(a). To address this issue, we employ an alternative parameter set for Au, obtained via Woods-Saxon parameter extraction that explicitly accounts for its nuclear deformation [13]. The results obtained with this new parameter set, shown in Fig. 2(b) show markedly improved agreement with the STAR data [19]. This highlights the critical role of detailed nuclear-structure information for the quantitative modeling of relativistic heavy-ion collisions.

The elliptic and triangular flow coefficients, v_2 and v_3 , characterize the hydrodynamic response of the quark-gluon plasma (QGP) to the corresponding initial-state spatial eccentricities, ε_2 and ε_3 , respectively, which are approximately related through the linear scaling $v_n \propto \varepsilon_n$ [49]. Within this framework, v_2 serves as a sensitive observable for investigating nuclear quadrupole deformation, while v_3 provides complementary sensitivity to nuclear octupole deformation. Figures 3(a) and (b) present the ratio of $v_3\{2\}^2$ for two distinct geometrical configurations of ^{238}U , evaluated with respect to the $\text{Au}_{\text{default}}$

and Au_{new} parameter sets, respectively. In the most central collision, the octupole-deformed configuration ($\text{U}_{\text{octupole}}$) with a non-vanishing β_{30} exhibits an enhancement of approximately 0.1 relative to the prolate configuration ($\text{U}_{\text{prolate}}$), as illustrated in Fig. 3(a). Furthermore, calculations performed with the Au_{new} parameter set confirm that this ~ 0.1 discrepancy persists, as shown in Fig. 3(b).

However, the absolute magnitudes differ substantially between the two Au parameter sets. The $\text{Au}_{\text{default}}$ parameters describes the STAR data [20] for all but the most central (0–2%) collisions. The Au_{new} parameter set yields improved agreement with the measurements in these most central (0–2%) collisions, but leads to an overestimation of the data at other centralities. The $R(v_3\{2\}^2)$ calculated under $\text{U}_{\text{octupole}}$ and $\text{Au}_{\text{default}}$ parameter sets (open red triangles) closely matches, both in overall trend and magnitude, the corresponding results for $\text{U}_{\text{prolate}}$ and Au_{new} parameter sets (blue squares) in the most central (0–2%) collisions, as illustrated in Fig. 3(b). This ambiguity is expected to induce a substantial systematic uncertainty in attempts to determine the pear-shaped (octupole) deformation of uranium using the v_3 observable. Our results indicate that the detailed nuclear structure of the reference system plays a crucial role when attempting to infer differences in nuclear shape solely from the comparison of flow observables across two collision systems.

Previous investigations have shown that, in addition to the elliptic flow v_2 , both the correlation coefficient $\langle v_2^2 \delta p_T \rangle$ and the mean transverse-momentum fluctuation $\langle (\delta p_T)^2 \rangle$ can serve as sensitive observables for constraining and extracting the quadrupole deformation of the colliding nuclei [19, 44–46]. We calculate the ratios of $\langle v_2^2 \delta p_T \rangle$ and $\langle (\delta p_T)^2 \rangle$ across different DFT configurations of ^{238}U and for two distinct parameter sets for Au, as presented in Fig. 4 and Fig. 5, respectively.

In Fig. 4, we note that the centrality-dependent trends of $\langle v_2^2 \delta p_T \rangle$ are in qualitative agreement with the experimental data. The two ^{238}U configurations show no significant differences for a given set of Au parameters. Quantitatively, all configurations and parameter sets lead to an overestimate of $\langle v_2^2 \delta p_T \rangle$, which can be attributed to the smaller effective Woods-Saxon quadrupole deformation parameter of ^{238}U obtained from the DFT calculations. We note that $\langle v_2^2 \delta p_T \rangle$ also exhibits sensitivity to the triaxial deformation of the colliding nuclei. In our analysis, we have kept the quadrupole deformation parameter fixed at $\beta_2^{\text{WS}} = -0.14$ for both sets of gold cases, noting that the quadrupole deformation of Au remains a major uncertainty in the initial conditions for $\text{Au} + \text{Au}$ collisions [13]. A preliminary investigation of ^{197}Au based on our CDFT calculations indicates a triaxial deformation characterized by the parameter $\gamma = 44^\circ$, which differs from the value $\gamma = 60^\circ$ adopted in the present analysis. Therefore, we expect that implementing the CDFT-motivated triaxial deformation for ^{197}Au will improve the precision of our predictions for $\langle v_2^2 \delta p_T \rangle$.

Figure 5 further illustrates the corresponding effect on the mean transverse-momentum fluctuation, $\langle (\delta p_T)^2 \rangle$. The model exhibits a systematic underestimation, with the primary contributors to this discrepancy being analogous to those identified for the $\langle v_2^2 \delta p_T \rangle$ observable. In particular, the CDFT calcula-

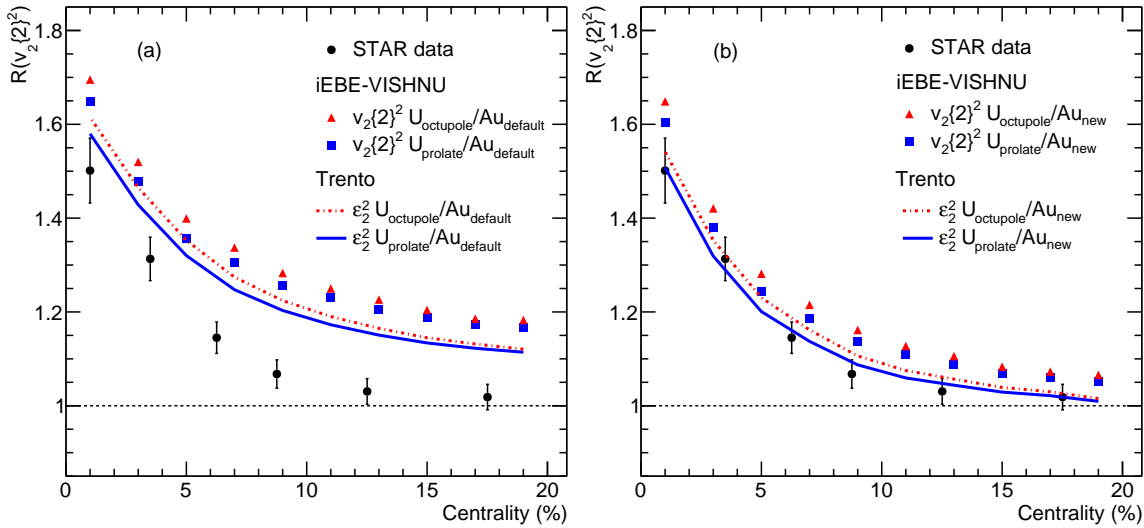


FIG. 2. (Color online) Centrality dependence of the $v_2^2\{2\}^2$ (or ε_2^2) ratio between U+U and Au+Au collisions obtained from iEBE-VISHNU (or initial TR_{ENT}O) simulations. The results in panels (a) and (b) are generated using the Au_{default} and Au_{new} parameter sets, respectively. Experiment data from the STAR Collaboration are taken from Ref. [19].

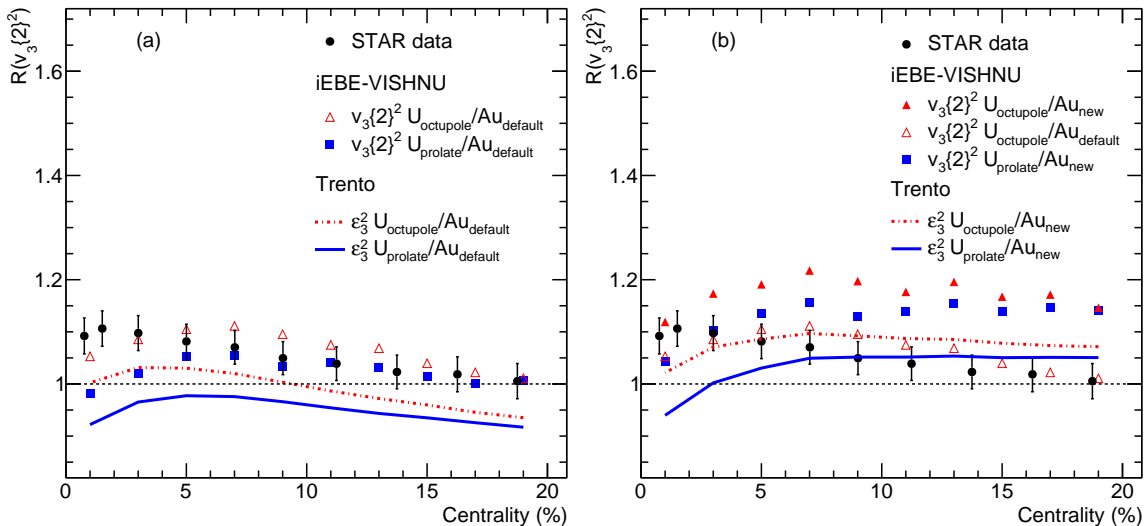


FIG. 3. (Color online) Centrality dependence of the $v_3^2\{2\}^2$ (or ε_3^2) ratio between U+U and Au+Au collisions obtained from iEBE-VISHNU (or initial TR_{ENT}O) simulations. The results in panels (a) and (b) are generated using the Au_{default} and Au_{new} parameter sets, respectively. Experiment data from the STAR Collaboration are taken from Ref. [20].

tions predict a reduced Woods-Saxon quadrupole deformation parameter for uranium, accompanied by a substantial hexadecapole deformation. One might expect these deviations to be reduced by using a spherical Au configuration, as is common in heavy-ion simulations; however, this would worsen the description of $R(\langle(\delta p_T)^2\rangle)$.

Our results demonstrate that precise knowledge of the Woods-Saxon parameters, particularly multipole deformation and surface diffuseness is essential to accurately model the initial conditions in heavy-ion collisions. We find that the centrality dependence of both $v_2\{2\}^2$ and $v_3\{2\}^2$, as well as multi-

particle observables such as $\langle v_2^2 \delta p_T \rangle$ and $\langle (\delta p_T)^2 \rangle$, is highly sensitive to these parameters. Adjusting the Au geometry from the commonly used set to one consistent with electron scattering data significantly reduces the overestimation of the v_2^2 ratio in the most central collisions, bringing hydrodynamic calculations closer to experimental measurements. However, this modification also leads to nontrivial and sometimes opposite effects on other observables such as the increasing magnitude of $R(v_3\{2\}^2)$, $R(\langle v_2^2 \delta p_T \rangle)$ and the decreasing magnitude of $R(\langle(\delta p_T)^2\rangle)$. Consequently, the tension between flow observables and transverse-momentum-related observables in their

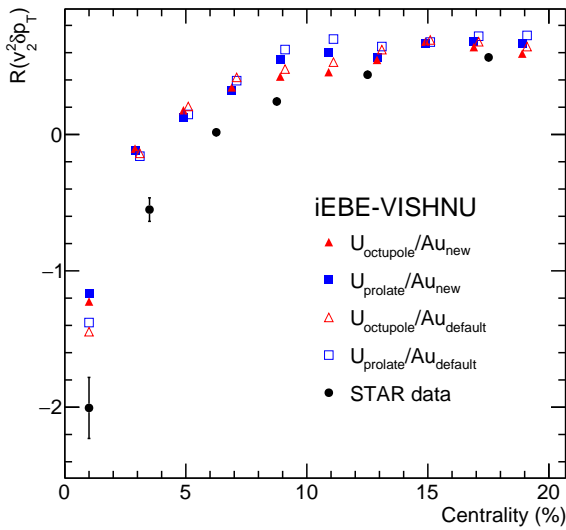


FIG. 4. (Color online) Centrality dependence of the $\langle v_2^2 \delta p_T \rangle$ ratio between U+U and Au+Au collisions, obtained from iEBE-VISHNU simulations. Experiment data from the STAR collaboration are taken from Ref. [19].

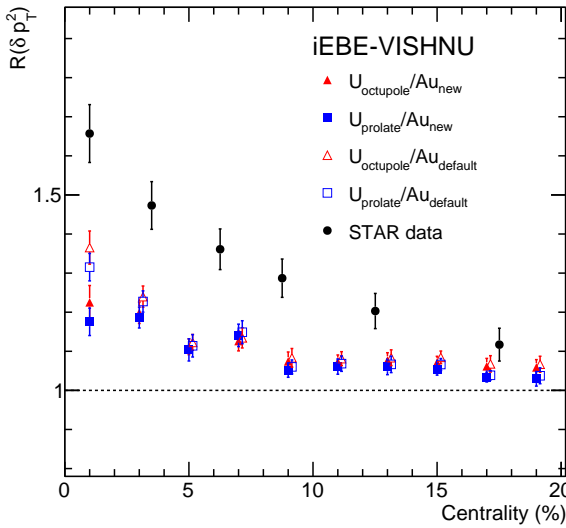


FIG. 5. (Color online) Centrality dependence of the $\langle (\delta p_T)^2 \rangle$ ratio between U+U and Au+Au collisions, obtained from iEBE-VISHNU simulations. Experiment data from the STAR Collaboration are taken from Ref. [19].

sensitivity to nuclear shape remains unresolved, as also shown in the recent STAR measurements reported in Ref. [19]. This discrepancy indicates the need for further refinement of heavy-ion collision models and the implementation of more realistic nuclear density distributions for Au. In this regard, recent measurements of $v_0(p_T)$ offer a promising avenue to investigate fluctuations and correlations in transverse momentum [50, 51]. Therefore, we plan to investigate these observables, as well as the more observable associated with nuclear multipole deformations, in future work by employing CDFT-based

nuclear density distributions for both ^{238}U and ^{197}Au in a subsequent study.

IV. SUMMARY

In this study, we employ event-by-event relativistic hydrodynamic simulations within the iEBE-VISHNU framework to investigate the impact of nuclear deformation on U+U and Au+Au collisions. The simulations incorporate uranium nuclear density distributions obtained from state-of-the-art calculations based on covariant density functional theory. Our results demonstrate that this state-of-the-art microscopic input produces a substantially enhanced characterization of the quadrupole deformation compared with conventional methodologies. In particular, the CDFT-based density provides an accurate reproduction of the experimentally observed ratio of elliptic flow coefficients $v_2^2\{2\}$ for the two collision systems, thereby offering a resolution of the previously reported “ultracentral v_2 puzzle” that arises when employing simplified Woods-Saxon parameterizations.

Nevertheless, in our analysis, the apparent inconsistency between different classes of observables persists. While the CDFT-based density profile successfully reproduces the measured flow anisotropy, a pronounced discrepancy arises when considering transverse-momentum-related observables. The single uranium configuration that accurately describes v_2 fails to simultaneously account for both the three-particle correlator $\langle v_2^2 \delta p_T \rangle$ and the event-by-event mean transverse momentum fluctuation $\langle (\delta p_T)^2 \rangle$. This tension points to a fundamental difficulty in how the effective quadrupole deformation of the initial state is encoded in different experimental probes, and it suggests that constraining the initial-state modeling solely through flow observables is inadequate for achieving a comprehensive description.

Furthermore, our analysis of the octupole deformation in uranium reveals an additional major challenge. Our CDFT calculations predict a substantial octupole deformation for ^{238}U . However, the extraction of β_3 from the triangular flow ratio $R(v_3\{2\}^2)$ proves to be highly sensitive to the assumed nuclear structure of ^{197}Au . We demonstrate that uncertainties in the Woods-Saxon diffuseness parameter for ^{197}Au can induce substantial variations in the relevant observables, thereby complicating the extraction of a clear and unambiguous experimental signature of the octupole deformation in uranium. Interdisciplinary collaborations that integrate realistic nuclear structure calculations with advanced heavy-ion modeling are essential to establish relativistic heavy-ion collisions as a precision tool for probing nuclear structure.

ACKNOWLEDGMENTS

This work is supported in part by the National Natural Science Foundation of China under Grants No. 12275082, No. 12147101 and No. 12325507, the National Key Research and Development Program of China under Grant No. 2022YFA1604900, and the Guangdong Major

Project of Basic and Applied Basic Research under Grant No. 2020B0301030008, and the Postdoctoral Fellowship Pro-

gram and China Postdoctoral Science Foundation under Grant Number BX20250170.

-
- [1] C. Golabek, A. C. C. Villari, S. Heinz, W. Mittig, S. Bhat-tacharyya, D. Boilley, G. de France, A. Drouart, L. Gaude-froy, L. Giot, A. Marchix, V. Maslov, M. Morjean, G. Mukherjee, A. Navin, Y. Penionzkevich, F. Rejmund, M. Rejmund, P. Roussel-Chomaz, and C. Stodel, Search for a long living giant system in $^{238}\text{U}+^{238}\text{U}$ collisions near the Coulomb barrier, *Int. J. Mod. Phys. E* **17**, 2235 (2008).
- [2] J. V. Kratz, M. Schädel, and H. W. Gäggeler, Reexamining the heavy-ion reactions $^{238}\text{U}+^{238}\text{U}$ and $^{238}\text{U}+^{248}\text{Cm}$ and actinide production close to the barrier, *Phys. Rev. C* **88**, 054615 (2013).
- [3] K. Zhao, Z. Li, N. Wang, Y. Zhang, Q. Li, Y. Wang, and X. Wu, Production mechanism of neutron-rich transuranium nuclei in $\text{U}^{238}+\text{U}^{238}$ collisions at near-barrier energies, *Phys. Rev. C* **92**, 024613 (2015).
- [4] K. Zhao, Z. Li, X. Wu, and Y. Zhang, Production probability of superheavy fragments at various initial deformations and orientations in the $^{238}\text{U}+^{238}\text{U}$ reaction, *Phys. Rev. C* **88**, 044605 (2013).
- [5] J. Tian, X. Wu, K. Zhao, Y. Zhang, and Z. Li, Properties of the composite systems formed in the reactions of $\text{U}-238 + \text{U}-238$ and $\text{Th}-232 + \text{Cf}-250$, *Phys. Rev. C* **77**, 064603 (2008).
- [6] C. Golabek and C. Simenel, Collision dynamics of two $\text{U}-238$ atomic nuclei, *Phys. Rev. Lett.* **103**, 042701 (2009), [arXiv:0904.3047 \[nucl-th\]](https://arxiv.org/abs/0904.3047).
- [7] K. Zhao, X. Wu, and Z. Li, The Study of Mass Distribution of products in 7.0-AMeV $^{238}\text{U}+^{238}\text{U}$ Collisions, *Phys. Rev. C* **80**, 054607 (2009), [arXiv:0910.5565 \[nucl-th\]](https://arxiv.org/abs/0910.5565).
- [8] K. Zhao, Z. Li, Y. Zhang, N. Wang, Q. Li, C. Shen, Y. Wang, and X. Wu, Production of unknown neutron-rich isotopes in $^{238}\text{U}+^{238}\text{U}$ collisions at near-barrier energy, *Phys. Rev. C* **94**, 024601 (2016), [arXiv:1605.07393 \[nucl-th\]](https://arxiv.org/abs/1605.07393).
- [9] B. Schenke, C. Shen, and P. Tribedy, Running the gamut of high energy nuclear collisions, *Phys. Rev. C* **102**, 044905 (2020), [arXiv:2005.14682 \[nucl-th\]](https://arxiv.org/abs/2005.14682).
- [10] G. Giacalone, J. Jia, and C. Zhang, Impact of Nuclear Deformation on Relativistic Heavy-Ion Collisions: Assessing Consistency in Nuclear Physics across Energy Scales, *Phys. Rev. Lett.* **127**, 242301 (2021), [arXiv:2105.01638 \[nucl-th\]](https://arxiv.org/abs/2105.01638).
- [11] N. Magdy, Impact of nuclear deformation on collective flow observables in relativistic $\text{U}+\text{U}$ collisions, *Eur. Phys. J. A* **59**, 64 (2023), [arXiv:2206.05332 \[nucl-th\]](https://arxiv.org/abs/2206.05332).
- [12] K. Hagino, N. W. Lwin, and M. Yamagami, Deformation parameter for diffuse density, *Phys. Rev. C* **74**, 017310 (2006), [arXiv:nucl-th/0604048](https://arxiv.org/abs/nucl-th/0604048).
- [13] Q. Y. Shou, Y. G. Ma, P. Sorensen, A. H. Tang, F. Videbæk, and H. Wang, Parameterization of Deformed Nuclei for Glauber Modeling in Relativistic Heavy Ion Collisions, *Phys. Lett. B* **749**, 215 (2015), [arXiv:1409.8375 \[nucl-th\]](https://arxiv.org/abs/1409.8375).
- [14] W. Ryssens, G. Giacalone, B. Schenke, and C. Shen, Evidence of Hexadecapole Deformation in Uranium-238 at the Relativistic Heavy Ion Collider, *Phys. Rev. Lett.* **130**, 212302 (2023), [arXiv:2302.13617 \[nucl-th\]](https://arxiv.org/abs/2302.13617).
- [15] H.-j. Xu, J. Zhao, and F. Wang, Hexadecapole Deformation of U^{238} from Relativistic Heavy-Ion Collisions Using a Nonlinear Response Coefficient, *Phys. Rev. Lett.* **132**, 262301 (2024), [arXiv:2402.16550 \[nucl-th\]](https://arxiv.org/abs/2402.16550).
- [16] Z. Wang, J. Chen, H.-j. Xu, and J. Zhao, Systematic investigation of the nuclear multipole deformations in $\text{U}+\text{U}$ collisions with a multi-phase transport model, *Phys. Rev. C* **110**, 034907 (2024), [arXiv:2405.09329 \[nucl-th\]](https://arxiv.org/abs/2405.09329).
- [17] G. Giacalone, Beyond axial symmetry: high-energy collisions unveil the ground-state shape of ^{238}U , *Nucl. Sci. Tech.* **35**, 218 (2024).
- [18] L. Adamczyk *et al.* (STAR), Azimuthal anisotropy in $\text{U}+\text{U}$ and $\text{Au}+\text{Au}$ collisions at RHIC, *Phys. Rev. Lett.* **115**, 222301 (2015), [arXiv:1505.07812 \[nucl-ex\]](https://arxiv.org/abs/1505.07812).
- [19] M. I. Abdulhamid *et al.* (STAR), Imaging shapes of atomic nuclei in high-energy nuclear collisions, *Nature* **635**, 67 (2024), [arXiv:2401.06625 \[nucl-ex\]](https://arxiv.org/abs/2401.06625).
- [20] Imaging nuclear shape through anisotropic and radial flow in high-energy heavy-ion collisions, *Rept. Prog. Phys.* **88**, 108601 (2025), [arXiv:2506.17785 \[nucl-ex\]](https://arxiv.org/abs/2506.17785).
- [21] M. Abdallah *et al.* (STAR), Search for the chiral magnetic effect with isobar collisions at $\sqrt{s_{NN}}=200$ GeV by the STAR Collaboration at the BNL Relativistic Heavy Ion Collider, *Phys. Rev. C* **105**, 014901 (2022), [arXiv:2109.00131 \[nucl-ex\]](https://arxiv.org/abs/2109.00131).
- [22] H.-J. Xu, X. Wang, H. Li, J. Zhao, Z.-W. Lin, C. Shen, and F. Wang, Importance of isobar density distributions on the chiral magnetic effect search, *Phys. Rev. Lett.* **121**, 022301 (2018), [arXiv:1710.03086 \[nucl-th\]](https://arxiv.org/abs/1710.03086).
- [23] S. Raman, C. W. G. Nestor, Jr, and P. Tikkanen, Transition probability from the ground to the first-excited 2+ state of even-even nuclides, *Atom. Data Nucl. Data Tabl.* **78**, 1 (2001).
- [24] D. Verney, History of the concept of nuclear shape, *Eur. Phys. J. A* **61**, 82 (2025).
- [25] S. Acharya *et al.* (ALICE), Characterizing the initial conditions of heavy-ion collisions at the LHC with mean transverse momentum and anisotropic flow correlations, *Phys. Lett. B* **834**, 137393 (2022), [arXiv:2111.06106 \[nucl-ex\]](https://arxiv.org/abs/2111.06106).
- [26] P. A. Butler and W. Nazarewicz, Intrinsic reflection asymmetry in atomic nuclei, *Rev. Mod. Phys.* **68**, 349 (1996).
- [27] T. Chupp, P. Fierlinger, M. Ramsey-Musolf, and J. Singh, Electric dipole moments of atoms, molecules, nuclei, and particles, *Rev. Mod. Phys.* **91**, 015001 (2019), [arXiv:1710.02504 \[physics.atom-ph\]](https://arxiv.org/abs/1710.02504).
- [28] D. D. Zhang, B. Li, D. Vretenar, T. Nikšić, Z. X. Ren, P. W. Zhao, and J. Meng, Ternary quasifission in collisions of actinide nuclei, *Phys. Rev. C* **109**, 024316 (2024), [arXiv:2310.02657 \[nucl-th\]](https://arxiv.org/abs/2310.02657).
- [29] P. Romatschke and U. Romatschke, Viscosity Information from Relativistic Nuclear Collisions: How Perfect is the Fluid Observed at RHIC?, *Phys. Rev. Lett.* **99**, 172301 (2007), [arXiv:0706.1522 \[nucl-th\]](https://arxiv.org/abs/0706.1522).
- [30] H. Song, S. A. Bass, U. Heinz, T. Hirano, and C. Shen, 200 A GeV $\text{Au}+\text{Au}$ collisions serve a nearly perfect quark-gluon liquid, *Phys. Rev. Lett.* **106**, 192301 (2011), [Erratum: *Phys. Rev. Lett.* 109, 139904 (2012)], [arXiv:1011.2783 \[nucl-th\]](https://arxiv.org/abs/1011.2783).
- [31] H.-j. Xu, Z. Li, and H. Song, High-order flow harmonics of identified hadrons in 2.76 A TeV $\text{Pb} + \text{Pb}$ collisions, *Phys. Rev. C* **93**, 064905 (2016), [arXiv:1602.02029 \[nucl-th\]](https://arxiv.org/abs/1602.02029).
- [32] W. Zhao, H.-j. Xu, and H. Song, Collective flow in 2.76 A TeV and 5.02 A TeV $\text{Pb}+\text{Pb}$ collisions, *Eur. Phys. J. C* **77**, 645 (2017), [arXiv:1703.10792 \[nucl-th\]](https://arxiv.org/abs/1703.10792).

- [33] J. Jia, Shape of atomic nuclei in heavy ion collisions, *Phys. Rev. C* **105**, 014905 (2022), arXiv:2106.08768 [nucl-th].
- [34] U. W. Heinz, H. Song, and A. K. Chaudhuri, Dissipative hydrodynamics for viscous relativistic fluids, *Phys. Rev. C* **73**, 034904 (2006), arXiv:nucl-th/0510014.
- [35] H. Song and U. W. Heinz, Causal viscous hydrodynamics in 2+1 dimensions for relativistic heavy-ion collisions, *Phys. Rev. C* **77**, 064901 (2008), arXiv:0712.3715 [nucl-th].
- [36] C. Shen, Z. Qiu, H. Song, J. Bernhard, S. Bass, and U. Heinz, The iEBE-VISHNU code package for relativistic heavy-ion collisions, *Comput. Phys. Commun.* **199**, 61 (2016), arXiv:1409.8164 [nucl-th].
- [37] J. E. Bernhard, J. S. Moreland, S. A. Bass, J. Liu, and U. Heinz, Applying Bayesian parameter estimation to relativistic heavy-ion collisions: simultaneous characterization of the initial state and quark-gluon plasma medium, *Phys. Rev. C* **94**, 024907 (2016), arXiv:1605.03954 [nucl-th].
- [38] S. A. Bass *et al.*, Microscopic models for ultrarelativistic heavy ion collisions, *Prog. Part. Nucl. Phys.* **41**, 255 (1998), arXiv:nucl-th/9803035.
- [39] M. Bleicher *et al.*, Relativistic hadron hadron collisions in the ultrarelativistic quantum molecular dynamics model, *J. Phys. G* **25**, 1859 (1999), arXiv:hep-ph/9909407.
- [40] J. S. Moreland, J. E. Bernhard, and S. A. Bass, Alternative ansatz to wounded nucleon and binary collision scaling in high-energy nuclear collisions, *Phys. Rev. C* **92**, 011901 (2015), arXiv:1412.4708 [nucl-th].
- [41] J. E. Bernhard, J. S. Moreland, and S. A. Bass, Bayesian estimation of the specific shear and bulk viscosity of quark-gluon plasma, *Nature Phys.* **15**, 1113 (2019).
- [42] A. Bilandzic, R. Snellings, and S. Voloshin, Flow analysis with cumulants: Direct calculations, *Phys. Rev. C* **83**, 044913 (2011), arXiv:1010.0233 [nucl-ex].
- [43] A. Bilandzic, C. H. Christensen, K. Gulbrandsen, A. Hansen, and Y. Zhou, Generic framework for anisotropic flow analyses with multiparticle azimuthal correlations, *Phys. Rev. C* **89**, 064904 (2014), arXiv:1312.3572 [nucl-ex].
- [44] G. Giacalone, Constraining the quadrupole deformation of atomic nuclei with relativistic nuclear collisions, *Phys. Rev. C* **102**, 024901 (2020), arXiv:2004.14463 [nucl-th].
- [45] J. Jia, S. Huang, and C. Zhang, Probing nuclear quadrupole deformation from correlation of elliptic flow and transverse momentum in heavy ion collisions, *Phys. Rev. C* **105**, 014906 (2022), arXiv:2105.05713 [nucl-th].
- [46] J. Jia, Probing triaxial deformation of atomic nuclei in high-energy heavy ion collisions, *Phys. Rev. C* **105**, 044905 (2022), arXiv:2109.00604 [nucl-th].
- [47] H. Li, H.-j. Xu, Y. Zhou, X. Wang, J. Zhao, L.-W. Chen, and F. Wang, Probing the neutron skin with ultrarelativistic isobaric collisions, *Phys. Rev. Lett.* **125**, 222301 (2020), arXiv:1910.06170 [nucl-th].
- [48] V. Koch, S. Schlichting, V. Skokov, P. Sorensen, J. Thomas, S. Voloshin, G. Wang, and H.-U. Yee, Status of the chiral magnetic effect and collisions of isobars, *Chin. Phys. C* **41**, 072001 (2017), arXiv:1608.00982 [nucl-th].
- [49] Z. Qiu and U. W. Heinz, Event-by-event shape and flow fluctuations of relativistic heavy-ion collision fireballs, *Phys. Rev. C* **84**, 024911 (2011), arXiv:1104.0650 [nucl-th].
- [50] G. Aad *et al.* (ATLAS), Evidence for the Collective Nature of Radial Flow in Pb+Pb Collisions with the ATLAS Detector, *Phys. Rev. Lett.* **136**, 032301 (2026), arXiv:2503.24125 [nucl-ex].
- [51] S. Acharya *et al.* (ALICE), Long-range transverse momentum correlations and radial flow in Pb–Pb collisions at the LHC, (2025), arXiv:2504.04796 [nucl-ex].